Shape analysis of brain ventricles using SPHARM

[1,2]G. Gerig, [1]M. Styner, [3]D. Jones, [3]D. Weinberger, [2]J. Lieberman

[1]Department of Computer Science
[2]Department of Psychiatry
University of North Carolina, Chapel Hill, NC 27599
[3]National Institute of Mental Health NIMH
Clinical Brain Disorders Branch, Bethesda, MD 20892
email: gerig@cs.unc.edu

Abstract

Enlarged ventricular size and/or asymmetry have been found markers for psychiatric illness, including schizophrenia. However, this morphometric feature is non-specific and occurs in many other brain diseases, and its variability in healthy controls is not sufficiently understood. We studied ventricular size and shape in 3D MRI (N=20) of monozygotic (N=5) and dizygotic (N=5) twin pairs. Left and right lateral, third and fourth ventricles were segmented from high-resolution T1w SPGR MRI using supervised classification and 3D connectivity. Surfaces of binary segmentations of left and right lateral ventricles were parametrized and described by a series expansion using spherical harmonics. Objects were aligned using the intrinsic coordinate system of the ellipsoid described by the first order expansion. The metric for pairwise shape similarity was the mean squared distance (MSD) between object surfaces. Without normalization for size, MZ twin pairs only showed a trend to have more similar lateral ventricles than DZ twins. After scaling by individual volumes, however, the pairwise shape difference between right lateral ventricles of MZ twins became very small with small group variance, differing significantly from DZ twin pairs. This finding suggests that there is new information in shape not represented by size, a property that might improve understanding of neurodevelopmental and neurodegenerative changes of brain objects and of heritability of size and shape of brain structures. The findings further suggest that alignment and normalization of objects are key issues in statistical shape analysis which need further exploration.

1 Introduction

Quantitative morphologic assessment of individual brain structures in neuroimaging most often includes segmentation followed by volume measurements. Volume changes are intuitive features as they might explain atrophy or dilation of structures due to illness. On the other hand, structural changes like bending/flattening or changes focused at a specific location of a structure, for example thickening of the occipital horn of ventricles, are not sufficiently reflected in global volume measurements. Development of new methods for three-dimensional shape analysis incorporating information about statistical biological variability aims at tackling this issue.

Davatzikos [1] proposed an analysis of shape morphometry via a spatially normalizing elastic transformation. Inter-subject comparisons were made by comparing the individual transformations. The method is applied in 2D to a population of corpora callosa. A similar approach in 3D has been chosen by Joshi et al [2] to compare hippocampi. Using the viscous fluid transformation proposed by Miller [3], inter-subject comparisons were made by analyzing the transformation fields. The *analysis* of transformation fields in both methods has to cope with the high dimensionality of the transformation and the sensitivity to the initial position. Although the number of subjects in the studied populations is low, both show a relatively stable extraction of shape changes (see Csernansky [4]). Quantitative analysis of shape changes provided by the deformation fields, expressed as point-wise changes in size, can be easily interpreted locally [5, 6]. A difficulty, however, is the inability of deformation fields to capture subtle changes that might be related to the various scales at which the object's geometric features are manifested.

The approach taken by Kelemen [7] evaluates a pop-

ulation of 3D hippocampal shapes based on a boundary description by spherical harmonic basis functions (SPHARM), which was proposed by Brechbühler [8, 9]. The SPHARM shape description delivers an implicit correspondence between shapes on the boundary, which is used in the statistical analysis. As in the approaches discussed before, this approach has to handle the problem of high dimensional features versus a low number of samples. Further, the detected shape changes are expressed as changes of coefficients that are hard to interpret.

Golland [10] in 2D and Pizer et al [11, 12] in 3D proposed two different approaches of applying shape analysis to a medial shape description. Blum [13] claims that medial descriptions are based on the idea of a biological growth model and a 'natural geometry for biological shape.' The medial axis in 2D captures shape intuitively and can be related to human vision (see Burbeck [14] and Siddiqui [15]). Both Pizer and Golland propose a sampled medial model that is fitted to individual shapes. By holding the topology of the model fixed, an implicit correspondence between shapes is given and statistical shape analysis can directlt be applied.

This paper applies a technique originally developed for model-based segmentation, the SPHARM shape representation of object surfaces [8, 7], to analyze brain structures. In particular, we address the clinical research problem of studying similarity of brain structures in idential (monozygotic, MZ) and non-identical (dizygotic, DZ) twin pairs. The paper is organized as follows. First we discuss the SPHARM description and its use for shape analysis, with special emphasis on the issues alignment and normalization of structures prior to measuring shape difference. We then present results of the lateral ventricle study in MZ/DZ twins.

2. Methods

2.1 Spherical harmonics (SPHARM)

In summary, the SPHARM description is a hierarchical, global, multi-scale boundary description that can only represent objects of spherical topology. The basis functions of the parameterized surface are spherical harmonics. Kelemen [7] demonstrated that SPHARM can be used to express shape deformations. Truncating the spherical harmonic series at different degrees results in object representations at different levels of detail. SPHARM is a smooth, accurate fine-scale shape representation, given a sufficiently small approximation error.

In the next sections, we briefly describe the mathematical properties of spherical harmonic descriptors, and the parameterization computation. Also, we discuss how to establish correspondence between different objects described

by SPHARM. This correspondence is used to compute the Mean Squared Distance (MSD) between surfaces, the metric for measuring shape difference used herein.

2.1.1 Spherical harmonics descriptors

This section gives a summary of spherical harmonic following Brechbühler [8].

Spherical harmonic basis functions Y_l^m, $-l \leq m \leq l$ of degree l and order m are defined on $\theta \in [0; \pi] \times \phi \in [0; 2\pi)$ by the following definitions [16] (see Fig. 1 left for a visualization of the basis function):

$$
\begin{aligned}
Y_l^m(\theta, \phi) &= \sqrt{\frac{2l+1}{4\pi} \frac{(l-m)!}{(l+m)!}} \, P_l^m(\cos\theta) \, e^{im\phi} \quad (1) \\
Y_l^{-m}(\theta, \phi) &= (-1)^m \, Y_l^{m*}(\theta, \phi) , \quad (2)
\end{aligned}
$$

where Y_l^{m*} denotes the complex conjugate of Y_l^m and P_l^m describes the associated Legendre polynomials

$$
P_l^m(w) = \frac{(-1)^m}{2^l \, l!}(1-w^2)^{\frac{m}{2}} \frac{d^{m+l}}{dw^{m+l}}(w^2-1)^l. \quad (3)
$$

To express a surface using spherical harmonics, the three coordinate functions are decomposed and the surface $\mathbf{v}(\theta, \phi) = (x(\theta, \phi), y(\theta, \phi), z(\theta, \phi))^T$ takes the form

$$
\mathbf{v}(\theta, \phi) = \sum_{l=0}^{\infty} \sum_{m=-l}^{l} \mathbf{c}_l^m \, Y_l^m(\theta, \phi) , \quad (4)
$$

where the coefficients $\mathbf{c}_l^m$ are three-dimensional vectors due to the three coordinate functions. The coefficients $\mathbf{c}_l^m$ are obtained by solving a least-squares problem. Therefore, the values of the basis functions are gathered in the matrix $\boldsymbol{z} = (z_{i,j(l,m)})$ with $z_{i,j(l,m)} = Y_l^m(\theta_i, \phi_i)$, where $j(l, m)$ is a function assigning an index to every pair (l, m) and i denotes the indices of the n_{vert} points to be approximated. The coordinates of these points are arranged in $\boldsymbol{v} = (\mathbf{v}_1, \mathbf{v}_2, \ldots, \mathbf{v}_{n_{vert}})^T$ and all coefficients are gathered in $\boldsymbol{c} = (\mathbf{c}_0^0, \mathbf{c}_1^{-1}, \mathbf{c}_1^0, \ldots)^T$. The coefficients that best approximate the points in a least-squares sense are obtained by

$$
\boldsymbol{c} = (\boldsymbol{z}^T\boldsymbol{z})^{-1}\boldsymbol{z}^T\boldsymbol{v} . \quad (5)
$$

Using spherical harmonic basis functions, we obtain a hierarchical surface description that includes further details as more coefficients are considered. This is illustrated in Fig. 1 right.

2.1.2 SPHARM description from voxel-based objects

The objects of interest are usually manually or semi-automatically segmented by a human expert, resulting in
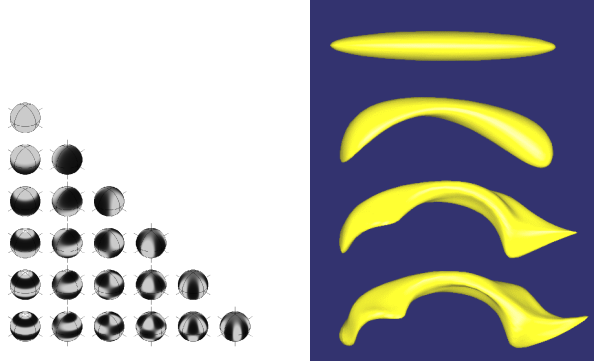
Figure 1. Decomposition of objects using SPHARM description. Left: Visualization of the Spherical harmonic basis functions. The plot shows the real parts of the spherical harmonic functions Y_l^m, with l growing from 0 (top) to 5 (bottom), and m ranging from 0 (left) to l in each row. Right: Description of a lateral ventricle (side view) at different degree's; m = 1,4,8,12 top to bottom.

a voxel representation. The voxel representation has to be preprocessed to fulfill the precondition of sphere topology, e.g. via a closing operation or a smoothing filter. As we are only interested in its boundary, the voxel representation is converted to a polygonal surface mesh that serves as input for the optimization procedure that finds an appropriate (θ_i, ϕ_i) parameterization [8].

The appropriate parameterization of the points of a surface description is a key problem. Every point i of the point cloud that will be approximated by the surface description is to be assigned a parameter vector (θ_i, ϕ_i). For surfaces of spherical topology, the natural parameter space is the unit sphere with polar coordinates. A homogeneous distribution of the parameter space is essential for the decomposition of the surface. This is also necessary for an appropriate approximation of corresponding points, as described in the next section 2.1.3.

A bijective mapping of the surface to the unit sphere is created, i.e., every point on the surface has to map to exactly one point on the sphere, and vice versa. The main idea of the procedure is to start with an initial parameterization. This initial parameterization is optimized so that every surface patch gets assigned an area in parameter space that is proportional to its area in object space, while the distortion to the quadrilateral mesh is minimized. The proposed parametrization of surfaces is invariant to object scaling as the whole surface is mapped to the unit sphere and optimized for homogeneous distribution of nodes.

2.1.3 SPHARM correspondence

The scheme for establishing correspondence between objects described by SPHARM [8] is a 3D extension of the 2D arc-length shape parameterization (see also Székely [17]). The first step is a homogeneous distribution of the parameter space over the surface, a step done in the parameterization optimization. In the second step the parameterization is rotated in the parameter space for normalization. This rotation is based on the first order ellipsoid, which is computed from the first three SPHARM coefficients. The result of the rotation satisfies the following properties:

- The parameter locations of the poles of the first order ellipsoid match with the poles of the sphere.

- The parameter locations of the 3 main ridges of the first order ellipsoid are moving along the equator, and the 0 and π meridians of the sphere.

Rotation in parameter space eliminates dependency of the parametrization from an arbitrary choice of poles of the surface parametrization. Correspondence between surfaces is know defined as the point-to-point correspondence established by points with the same parameter vector (θ_i, ϕ_i). Whereas alignment and rotation in parameter space is thus normalized on a coarse scale object representation (ellipsoid), the final correspondence is obtained by expansion of the object to a higher degree. The quality of the correspondence is shown in Fig. 2. The visual comparison demonstrates that normalizing the parameter space on a coarse scale description of objects results a good correspondence despite the fact that it does not use explicit characteristic surface features. A quantitative evaluation study against manual landmarking is currently in progress. Please note that objects shown in Fig. 2 have been spatially normalized as described in later section 2.2.

2.1.4 Mean Squared Distance (MSD) between SPHARM objects

The correspondence between objects described by SPHARM allows the computation of distance measures between two objects. The orthogonality of the spherical harmonic basis functions allows Parseval's theorem to be used to compute the root Mean Squared Distance ($\sqrt{MSD}$) between two objects directly from their coefficients via a difference calculation. A correction is needed since the squared spherical harmonic basis functions do not integrate to 1 but to 4π.

$$MSD = \frac{1}{4\pi} \cdot \sum_{l=0}^{\inf} \sum_{m=-l}^{l} ||\mathbf{c}_{1,l}^m - \mathbf{c}_{2,l}^m||^2 \qquad (6)$$
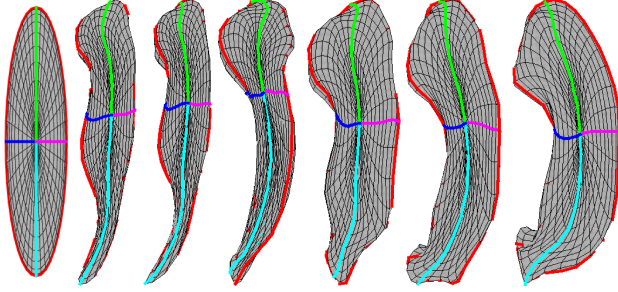
Figure 2. Visualization of the SPHARM correspondence. A first order ellipsoid and six left lateral ventricles are displayed. The surface net shows the (θ_i, ϕ_i) parameterization (same parameters = same homologous points). The ridges on the first order ellipsoid are the equator and $\{0, \pi/2, \pi, 3 \cdot \pi/2\}$ meridian lines in all objects. The equator and meridian lines are emphasized in different colors. The poles are at the crossing of the meridian lines.

Error measures other than $\sqrt{MSD}$ need an appropriate sampling of the spherical parameterization (θ_i, ϕ_i), for example by an iterative icosahedron subdivision of the spherical (θ, ϕ) parameter space. Using the point-to-point correspondence described previously and this sampling, error measures like the Mean Absolute Distance (MAD), Hausdorff-distance or arbitrary quantiles derived from the histogram of surface distances can be computed straightforwardly.

2.2 Object alignment and scaling

As a prerequisite for any shape similarity calculation, shapes have to be normalized with respect to a reference coordinate frame. Since we are interested in measuring shape differences, a normalization is needed to eliminate differences that are due to rotation, translation and magnification. Normalization of translation and rotation is accomplished by aligning the SPHARM objects via the first order ellipsoid. This perfectly matches center and axes of the first order ellipsoids (see Fig. 3).

In order to normalize for magnification, an appropriate scaling method has to be defined. The choice of the scaling method depends on the task and the type of objects. We investigated two possibilities:

A No scaling correction: The computation of shape differences without any scale normalization reveals differences between small and large objects even though they might have the same shape properties. Thus, the

differences will reflect mixed values of both the shape differences and the size differences.

B Uniform scaling to unit volume: Creating a shape difference measure that is orthogonal in its nature to the volume measure has the potential to reveal information additional to size. The volume measurements can be incorporated later into a multivariate statistical analysis as an additional orthogonal feature (see later Fig 8).

The effects of the two different scalings applied to the driving clinical problem are illustrated in Fig. 3.

Alignment

No scaling   Unit Volume scaling
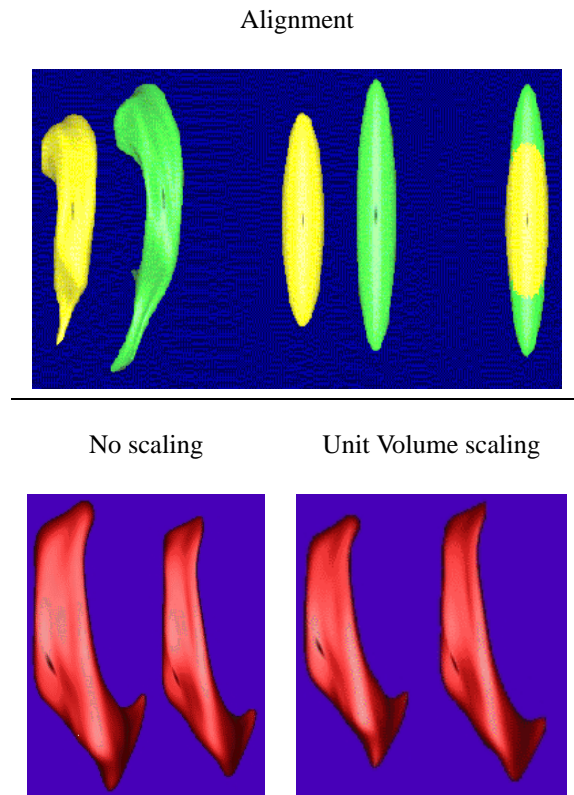
Figure 3. Object alignment and scaling. Top row: Two left lateral ventricles are aligned to perfectly match the center and axis of the first order ellipsoid; left: objects, middle: first order ellipsoids, right: aligned ellipsoids. Bottom row: Pairs of right lateral ventricles (MZ twin pair) unscaled (left) and scaled to unit volume (right). This example shows that shapes are quite similar and that the scaling corrected for an existing size difference.

3. Results

This section presents SPHARM applied to a population of lateral ventricles, a fluid filled structure in the center of the human brain that is divided into a left and a right part located in the respective brain hemispheres. The image data is part of a mono/dizygotic twin study and consists of 20 twin subjects (10 pairs, 5 monozygotic and 5 dizygotic pairs). The original brain images were provided by D. Weinberger, NIMH Neuroscience in Bethesda, Maryland. The segmentation method used a single gradient-echo channel (T1w, 256x256x128, 240mm FOV, 1.5mm slice distance) with manual seeding for Parzen-window based non-parametric supervised statistical classification. Manually-guided three-dimensional connectivity was used to extract the left and right lateral ventricles. The segmented structures were post-processed using a closing operation with a spherical structuring element of radius of two voxels to provided simply connected 3D objects as required for surface parametrization.
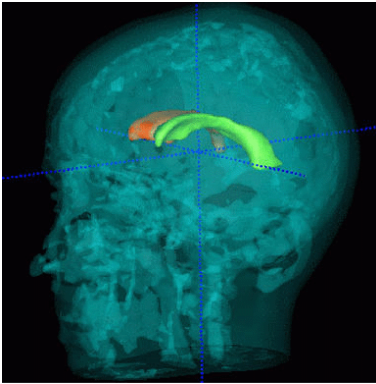
Figure 4. Three-dimensional rendering of the skin surface (transparent) and the lateral ventricles. Lateral ventricle of left and right brain hemispheres are shown in green and orange.

Fig. 5 displays the lateral ventricles of all twin pairs. The statistical shape analysis presented below aimed to distinguish monozygotic (MZ) twins from dizygotic (DZ) twins and from unrelated pairs. The three subject groups are matched for age, gender and handedness. The population size of each group is very small (5 MZ, 5DZ, 10 unrelated), so the observed effect must be quite large for the statistical analysis to yield a significant result. A previous study was performed by Bartley et al [18] on the same datasets with the goal of distinguishing the populations. They compared cortical gyral patterns and the total brain volumes. Both measures show significant differences between the MZ and DZ populations.
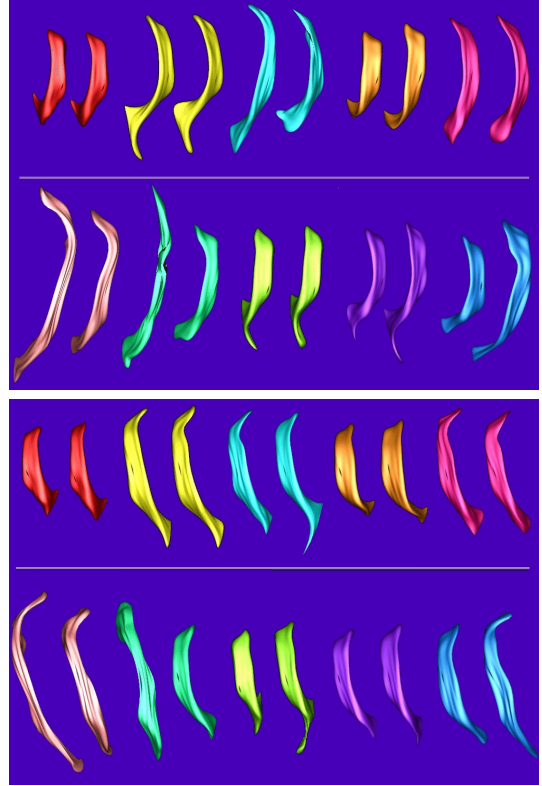
Figure 5. Visualization of the lateral ventricles of all twin pairs (same color for pairs) scaled with the individual volume (correct relative size). Top two rows: Left ventricles. Bottom two rows: Right ventricles. Each block: Top row: MZ twins. Bottom Row: DZ twins.

3.1 Volume similarity analysis

We studied the twin pair's similarity using signed volume difference but also normalized absolute volume difference: $\Delta vol_{T_{1,2}} = |vol_{T_1} - vol_{T_2}|/(vol_{T_1} + vol_{T_2})$. The former uses volumes normalized by individual size of intracranial cavity, whereas the latter is a relative measure and independent of overall brain size. We will only discuss the relative measure as the absolute measure presented significantly more population noise. As shown in Fig. 6, there is a trend in both brain hemispheres between the two populations, but no significant conclusions can be drawn since the volume measurement distributions are overlapping. The p-values for discriminating the two population are at 0.15 and 0.16, which is non-significant at a 5% significance level (see Tab. 1).

5
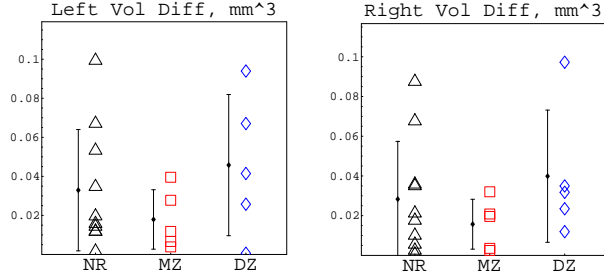
Figure 6. Plot of pairwise relative ventricle volume difference $\Delta vol_{T_{1,2}}$ between MZ and DZ twin groups. Results of left and right ventricles are shown in the left and right figures. No significant conclusions can be drawn.

3.2 Shape analysis via SPHARM

The SPHARM coefficients of the objects were determined and normalized with respect to rotation and translation using the first order ellipsoid. Using the objects not normalized for scaling, our analysis yields no significant difference between the two populations as shown in Fig. 7 and Table 1. There is just a trend showing a smaller volume difference in MZ pairs versus DZ pairs. A significant difference between MZ and DZ groups is observed for the lateral ventricles in the right brain hemisphere after normalizing (isotropic scaling) the objects for individual volumes. The p-value is at 0.019 (see Tab. 1), which suggests significance at the 5% level.

	MZ/DZ	MZ/Other	DZ/Other
Volume Left	0.151	0.333	0.486
Volume Right	0.167	0.377	0.500
MSD unscaled Left	0.201	**0.030**	0.295
MSD unscaled Right	0.145	**0.042**	0.419
MSD scaled Left	0.106	**0.046**	0.825
MSD scaled Right	**0.019**	**0.009**	0.471

Table 1. Table of p-values for discriminating the 3 populations of MZ and DZ twin pairs and unrelated pairs. Bold numbers are significant at the 5% level.

A closer analysis of the results plotted in Figure 7 reveals interesting new information about the structure of brain ventricles in genetically identical MZ twin pairs, non-identical DZ twins, and non-related but age and gender matched pairs. We are well aware that we have to be cautious with conclusions due to the small sample size. Before size nor-

malization (upper row), the left and right ventricles show the same trend, namely that MZ twins are more similar than DZ twins. Group tests were not significant which is in part due to the small sample size. After size normalization with individual volumes, the right ventricles reveal a very interesting result. MZ twin pairs show a very small shape difference and very low variability, suggesting that the shapes after normalization are very similar (see also Fig. 5). This shows that differences of right ventricles in MZ twin pairs are mostly due to a global scaling (see Fig. 6) and that there are only minor residual shape differences. Surprisingly, this strong and significant effect is not found for the left ventricles, where even after size normalization there is only a trend showing more similar ventricle shapes in MZ as compared to DZ. The statistics further illustrates that DZ twin pairs didn't differ from unrelated pairs, both before and after volume normalization.
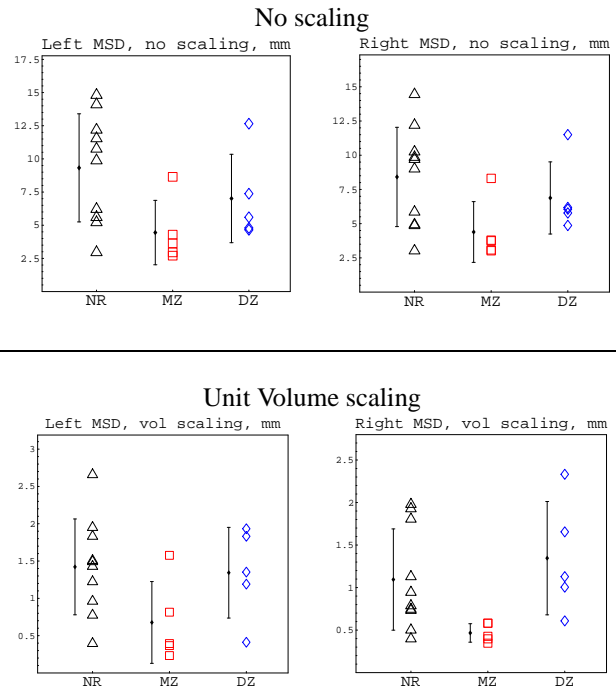
Figure 7. Plot of MSD shape difference between twins of the left (left column) and right (right column) lateral ventricles. Top row: Plots for shape difference when no scaling normalization is applied. Bottom row: Plots when objects are isotropically scaled to unit volume. The vertical axis displays the MSD shape difference in mm.

The splitting of size difference and residual shape difference between pairs allows us to use both measures in a

combined analysis, as there might be an interaction between volume and shape differences leading to a better group discrimination or an improved understanding of morphologic differences. Figure 8 illustrates the two-dimensional feature space with relative volume difference (vertical axis) and MSD shape difference of size-normalized objects (horizontal axis) for the left and right ventricles. The three groups unrelated subjects (NR), MZ twins and DZ twins are indicated by triangles, squares and diamonds. Interpretation is difficult due to the small sample size and the non-Gaussian distribution of samples, suggesting that multi-variate non-parametric statistical techniques would be required for a quantitative analysis. A visual comparison shows that discrimination between MZ and DZ twin pairs is better for the right ventricles than for the left ventricles. Discrimination, however, would be mostly governed by the MSD shape difference measure rather than the volume difference measure.
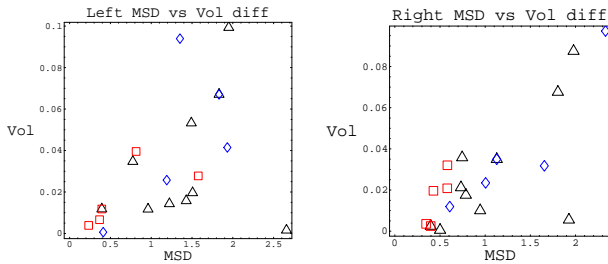
Figure 8. Plot of combined MSD shape difference and volume difference between twins of the left (left column) and right (right column) lateral ventricles. MZ Twins are shown as red squares, DZ Twins as blue diamonds and unrelated subjects (NR) as black triangles. Lateral ventricles were scaled to unit volume for the MSD shape difference measure.

4. Conclusions

This paper presents shape analysis using surface parametrization by spherical harmonics. The hierarchical nature of the SPHARM shape representations allows object alignment by an intrinsic coordinate system derived from a coarse scale representation, which is feasible for objects depicting three distinctly different major axis. Previous work [8, 7] and results presented in this paper demonstrate that this alignment results in a good initial point-to-point correspondence of surfaces if shapes are derived from a homogeneous shape population. A quantitative analysis of the quality of 3D correspondence is the subject of a current study. The method presented herein can be seen

as complimentary to the seminal work by Toga et al. [5, 6] as it does not express shape variability in Talairach stereotaxic space but an an intrinsic object-centered coordinate system. The shape distance metric used herein is equivalent to the mean square distance (MSD) between densly sampled corresponding surface points, however obtained by a quick calculation in parameter space. Alternative shape representation schemes providing dense sets of corresponding points could be used as well. The MSD is known to be sensitive to outliers. Future work will replace the MSD metric by statistical analysis of quantiles derived from surface distance histograms as discussed in the text.

The MZ/DZ twin study demonstrates that shape measures reveals new information additional to size measurements which might become relevant for improved understanding of structural differences in normal populations but also in comparisons between healthy controls and patients. Twin studies offer the advantage to reduce natural biological variability by choosing subjects with identical genes. This study clearly demonstrates that significant differences between MZ and DZ pairs could not be found by volume measurements but only by analyzing shape. Scaling by volume showed that there is only a minor residual shape difference for the right but not for the left ventricle, and that this lateralized shape effect results in a significant group difference between MZ and DZ twin pairs. We have no obvious explanation for this finding but hope to get more insight through close collaboration with experts in neurobiology and neurodevelopment. Global scaling reveals an effect otherwise hidden due to the fact that any size change would also be reflected in the shape difference measure. The choice of scaling might depend on the application domain and on the type of shape effects to be studies. Alternative choices would include the size of the longest axis, an affine transformation, or a Procrustes fit between sets of corresponding points. A follow-up study currently analyzes differences between MZ twins discordant for schizophrenia to reveal insight into hypothesized morphologic changes due to illness. Analysis of shape changes similarly to the case study presented here might also become important in longitudinal assessments of morphologic change due to developmental or degenerative processes.

A weakness of shape analysis by SPHARM is the non-intuitive nature of the set of coefficients describing shape. Shape difference findings, even found to be statistically significant, do not easily reveal the type and localization of the effect. Localized shape differences between groups are only qualitatively accessible by 3D surface renderings labeled with results of local test statistics (e.g. [4]) or by cine loops displaying a morphing between mean shapes. The important issue of providing an intuitive shape description expressed in terms of natural language, e.g. change of width or curvature) are currently addressed by developing an alter-

native shape representation technique based on 3D medial representations (skeletons) [19, 20].

Acknowledgements

References

[1] C. Davatzikos, M. Vaillant, S. Resnick, J.L Prince, S. Letovsky, and R.N. Bryan, "A computerized method for morphological analysis of the corpus callosum," *J. of Comp. Ass. Tomography.*, vol. 20, pp. 88–97, Jan./Feb 1996.

[2] S. Joshi, M Miller, and U. Grenander, "On the geometry and shape of brain sub-manifolds," *Pattern Recognition and Artificial Intelligence*, vol. 11, pp. 1317–1343, 1997.

[3] G.E. Christensen, R.D. Rabbitt, and M.I. Miller, "3d brain mapping using a deformable neuroanatomy," *Physics in Medicine and Biology*, vol. 39, pp. 209–618, 1994.

[4] J.G. Csernansky, S. Joshi, L.E. Wang, J. Haller, M. Gado, J.P. Miller, U. Grenander, and M.I. Miller, "Hippocampal morphometry in schizophrenia via high dimensional brain mapping," *Proc. Natl. Acad. Sci. USA*, vol. 95, pp. 11406–11411, September 1998.

[5] A.W. Toga and P.M. Thompson, "The role of image registration in brain mapping," *Image and Vision Computing*, vol. 19, pp. 3–24, 2001.

[6] K.L. K.L. Narr, P.M. Thompson, T. Sharma, J. Moussai, R.E. Blanton, B. Anvar, A. Edris, R. Krupp, J. Rayman, M. Khaledy, and A.W. Toga, "3d mapping of temporo-limbic regions and the lateral ventricles in schizophrenia," *Biological Psychiatry*, vol. 50, pp. 84–97, 2001.

[7] G. Kelemen, A.and Székely and G. Gerig, "Elastic model-based segmentation of 3d neuroradiological data sets," *IEEE Trans. Med. Imaging*, vol. 18, pp. 828–839, October 1999.

[8] C. Brechbühler, G. Gerig, and O. Kübler, "Parametrization of closed surfaces for 3-D shape description," *CVGIP: Image Under.*, vol. 61, pp. 154–170, 1995.

[9] C. Brechbühler, *Description and Analysis of 3-D Shapes by Parametrization of Closed Surfaces*, 1995, Diss., IKT/BIWI, ETH Zürich, ISBN 3-89649-007-9.

[10] P. Golland, W.E.L. Grimson, and R. Kikinis, "Statistical shape analysis using fixed topology skeletons: Corpus callosum study," in *Inf. Proc. in Med. Imaging*, 1999, pp. 382–388.

[11] S. Pizer, D. Fritsch, P. Yushkevich, V. Johnson, and E. Chaney, "Segmentation, registration, and measurement of shape variation via image object shape," *IEEE Trans. Med. Imaging*, vol. 18, pp. 851–865, Oct. 1999.

[12] M. Styner and G. Gerig, "Medial models incorporating shape variability," in *Inf. Proc. in Med. Imaging*, 2001, pp. 502–516.

[13] T.O. Blum, "A transformation for extracting new descriptors of shape," in *Models for the Perception of Speech and Visual Form*. 1967, MIT Press.

[14] C.A. Burbeck, S.M. Pizer, B.S. Morse, D. Ariely, G. Zauberman, and J Rolland, "Linking object boundaries at scale: a common mechanism for size and shape judgements," *Vision Research*, vol. 36, pp. 361–372, 1996.

[15] K. Siddiqi, B. Kimia, S. Zucker, and A. Tannenbaum, "Shape, shocks and wiggles," *Image and Vision Computing Journal*, vol. 17, pp. 365–373, 1997.

[16] W. H. Press, S. A. Teukolsky, W. T. Vetterling, and B. P. Flannery, *Numerical Recipes in C*, Cambridge Univ. Press, 2 edition, 1993.

[17] G. Székely, A. Kelemen, Ch. Brechbühler, and G. Gerig, "Segmentation of 2-D and 3-D objects from MRI volume data using constrained elastic deformations of flexible Fourier contour and surface models," *Medical Image Analysis*, vol. 1, no. 1, pp. 19–34, 1996.

[18] A. Bartley, D. Jones, and D. Weinberger, "Genetic variability of human brain size and cortical patterns," *Brain*, vol. 120, pp. 257–269, 1997.

[19] P. Yushkevich and S. Pizer, "Coarse to fine shape analysis via medial models," in *Inf. Proc. in Med. Imaging*, 2001, LNCS 2082, pp. 402–408.

[20] G. Gerig and M. Styner, "Shape versus size: Improved understanding of the morphology of brain structures," in *Medical Image Computing and Computer-Assisted Intervention*, 2001, accepted for publication.